

2022

A Fundamental Equation of State for trans-1,1,1,4,4,4-Hexafluoro-2-butene [R1336mzz(E)]

Ryo Akasaka

Luke D. Simoni

Eric W. Lemmon

Follow this and additional works at: <https://docs.lib.purdue.edu/iracc>

Akasaka, Ryo; Simoni, Luke D.; and Lemmon, Eric W., "A Fundamental Equation of State for trans-1,1,1,4,4,4-Hexafluoro-2-butene [R1336mzz(E)]" (2022). *International Refrigeration and Air Conditioning Conference*. Paper 2314.
<https://docs.lib.purdue.edu/iracc/2314>

This document has been made available through Purdue e-Pubs, a service of the Purdue University Libraries. Please contact epubs@purdue.edu for additional information. Complete proceedings may be acquired in print and on CD-ROM directly from the Ray W. Herrick Laboratories at <https://engineering.purdue.edu/Herrick/Events/orderlit.html>

A Fundamental Equation of State for *trans*-1,1,1,4,4,4-Hexafluoro-2-butene [R1336mzz(E)]

Ryo AKASAKA^{1*}, Luke D. SIMONI², Eric W. LEMMON³

¹ Department of Mechanical Engineering, Faculty of Science and Engineering, Kyushu Sangyo University, 2-3-1 Matsukadai, Higashi-ku, Fukuoka 8138503, Japan (ryo-a@ip.kyusan-u.ac.jp)

² The Chemours Company, Fluorochemicals Technology, Newark, Delaware 19713, USA (Luke.D.Simoni@chemours.com)

³ Applied Chemicals and Materials Division, National Institute of Standards and Technology, 325 Broadway, Boulder, Colorado 80305, USA (eric.lemmon@nist.gov)

* Corresponding Author

ABSTRACT

A fundamental equation of state expressed explicitly in the Helmholtz energy is presented for *trans*-1,1,1,4,4,4-hexafluoro-2-butene [R1336mzz(E)]. Although the equation is based on limited experimental data, its expected uncertainties are small enough for most engineering applications. In addition, the equation exhibits reasonable behavior in the critical and extrapolated regions. The equation is an interim model, but it is the best currently available property representation for R1336mzz(E).

1. INTRODUCTION

The substance *trans*-1,1,1,4,4,4-hexafluoro-2-butene (CAS No. 66711-86-2), also known as R1336mzz(E), is considered one of the next-generation refrigerants due to its zero-ozone depletion potential with an ultra-low GWP, non-flammability, and its favorable thermophysical properties. Its non-flammable characteristic offers the possibility of large-scale waste-heat recovery applications such as high-temperature heat pumps and organic Rankine cycles (Juhasz, 2017; Murphy & Katancik, 2021). The refrigerant blend R471A, a ternary mixture of 78.7 mass% *trans*-1,3,3,3-tetrafluoroprop-1-ene [R1234ze(E)], 4.3 mass% 1,1,1,2,3,3,3-heptafluoropropane (R227ea), and 17.0 mass% R1336mzz(E), is considered as a potential alternative to 1,1,1,2-tetrafluoroethane (R134a). The fundamental properties of R1336mzz(E) are summarized in Table 1.

Table 1: Fundamental properties of R1336mzz(E)

Property	Value	Reference
CAS number	66711-86-2	
Chemical formula	<i>trans</i> -CF ₃ CH=CHCF ₃	
Molar mass	164.06 g mol ⁻¹	Kayukawa <i>et al.</i> (2021)
Critical temperature	403.53 K	Sakoda <i>et al.</i> (2020)
Critical pressure	2.7790 MPa	This work
Critical density	3.129 mol dm ⁻³	This work
Triple-point temperature	200.15 K	Tomassetti <i>et al.</i> (2022)
Normal boiling-point temperature	281.02 K	This work
Acentric factor	0.413	This work
Total lifetime	0.334 yrs	Kayukawa <i>et al.</i> (2021)
GWP (100-yr)	16	Kayukawa <i>et al.</i> (2021)

Although thermodynamic property data for R1336mzz(E) are scarce, Sakoda *et al.* (2020) recently made extensive measurements of the critical parameters, vapor pressures, saturated liquid and vapor densities, and (p, ρ, T) behavior in both liquid and vapor phases. The work here developed a Helmholtz energy equation of state by mainly fitting the experimental data of Sakoda *et al.* This equation was successfully employed in subsequent studies on transport properties and heat transfer analysis for R1336mzz(E) (Kedzierski & Lin, 2020; Mondal *et al.*, 2021, 2022). This paper presents the outline of the formulation of the equation of state and demonstrates comparisons to experimental data and behavior at critical and extrapolated regions. More detailed discussions are given elsewhere (Akasaka *et al.*, 2022).

2. EQUATION OF STATE

The equation of state for R1336mzz(E) was formulated with the Helmholtz energy as the fundamental property with independent variables of temperature and density, which has the form

$$\frac{a(T, \rho)}{RT} = \alpha(\tau, \delta) = \alpha^\circ(\tau, \delta) + \alpha^r(\tau, \delta), \quad (1)$$

where $R = 8.314462618 \text{ J mol}^{-1} \text{ K}^{-1}$ is the molar gas constant (Tiesinga *et al.*, 2021), a is the molar Helmholtz energy, α is the dimensionless Helmholtz energy, $\tau = T_c/T$ is the reciprocal reduced temperature, and $\delta = \rho/\rho_c$ is the reduced density. The critical temperature T_c is 403.53 K, which is the experimental value determined by Sakoda *et al.* (2020). The critical density ρ_c is $3.129 \text{ mol dm}^{-3}$, and it was determined while the fitting in this work starting from the experimental value by Sakoda *et al.* (2020) ($513 \text{ kg m}^{-3} \approx 3.127 \text{ mol dm}^{-3}$). Sakoda *et al.* (2020) experimentally determined the critical pressure as 2.7792 MPa, and the equation of state calculates it as 2.7790 MPa at 403.53 K and $3.129 \text{ mol dm}^{-3}$.

The dimensionless Helmholtz energy α is split into an ideal-gas part α° representing ideal-gas properties and a residual part α^r corresponding to the influence of intermolecular forces. They are normally individually formulated. According to the ideal-gas law, the dimensionless ideal-gas Helmholtz energy α° is analytically derived from an equation for the isobaric heat capacity:

$$\alpha^\circ(\tau, \delta) = \frac{h_0^\circ \tau}{RT_c} - \frac{s_0^\circ}{R} - 1 + \ln \frac{\delta \tau_0}{\delta_0 \tau} - \frac{\tau}{R} \int_{\tau_0}^{\tau} \frac{c_p^\circ}{\tau^2} d\tau + \frac{1}{R} \int_{\tau_0}^{\tau} \frac{c_p^\circ}{\tau} d\tau, \quad (2)$$

where $\tau_0 = T_c/T_0$, $\delta_0 = \rho_0/\rho_c = p_0/(RT_0\rho_c)$, T_0 is the temperature at a reference state, p_0 is a reference pressure for the ideal-gas properties, and ρ_0 is the ideal-gas density at T_0 and p_0 . The Planck-Einstein form is used in this work to formulate the c_p° equation, which is given by

$$\frac{c_p^\circ}{R} = n_0^\circ + \sum_{i=1}^2 n_i^\circ \left(\frac{m_i^\circ}{T} \right)^2 \frac{\exp(m_i^\circ/T)}{[\exp(m_i^\circ/T) - 1]^2}. \quad (3)$$

The coefficients m_i° and n_i° were initially determined from the experimental c_p° data of Kano *et al.* (2019) and further adjusted while subsequently fitting vapor-phase sound speed data. The dimensionless residual Helmholtz energy α^r is given by

$$\alpha^r(\tau, \delta) = \sum_{i=1}^5 N_i \tau^i \delta^{d_i} + \sum_{i=6}^{10} N_i \tau^i \delta^{d_i} \exp(-\delta^i) + \sum_{i=11}^{15} N_i \tau^i \delta^{d_i} \exp[-\eta_i(\delta - \varepsilon_i)^2 - \beta_i(\tau - \gamma_i)^2]. \quad (4)$$

This form is basically empirical, and the number of terms and the coefficients and exponents are generally determined by fitting experimental data. The nonlinear least-square fitting technique originally developed by Lemmon *et al.* (2009) was used in this work, where various thermodynamic constraints were also applied to ensure physically correct behavior over wide ranges of temperature and pressure. The constraints are discussed in our recent papers (Akasaka & Lemmon, 2019; Akasaka *et al.*, 2020). The final values for the coefficients and exponents in Eqs. (3) and (4) are given elsewhere (Akasaka *et al.*, 2022).

3. COMPARISON TO EXPERIMENTAL DATA

3.1 Vapor Pressure

Figure 1 shows relative deviations and absolute differences between experimental vapor pressures and calculated values with the equation of state. Four datasets are currently available for the vapor pressures of R1336mzz(E). The

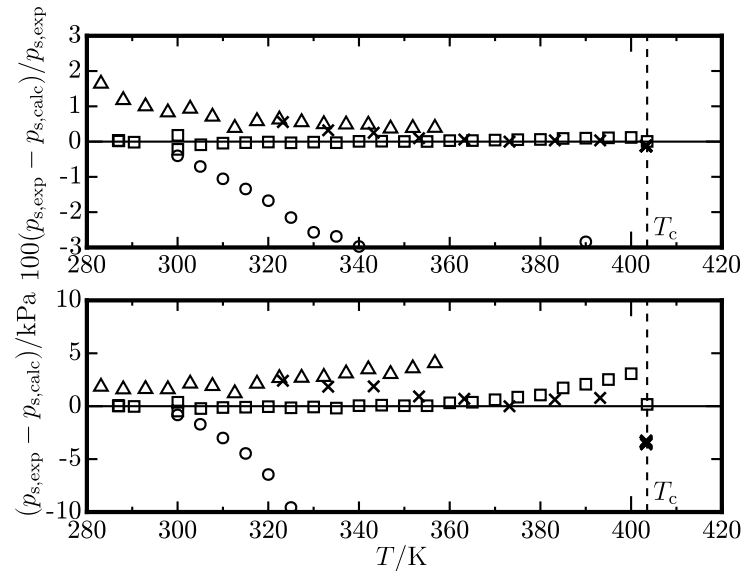


Figure 1: Relative deviations (top panel) and absolute differences (bottom panel) between experimental vapor pressures and calculated values with the equation of state: (×) Tanaka *et al.* (2017); (○) Kimura (2019); (□) Sakoda *et al.* (2020); (Δ) Boonaert *et al.* (2020)

data of Sakoda *et al.* (2020) are located at temperatures from 287 K to the critical temperature; they are accurately represented with an average deviation of 0.05 %. The maximum difference between experimental and calculated values is 3.1 kPa at 400 K, which is larger than the experimental uncertainty (1 kPa, $k = 2$) but acceptable in most engineering applications. The data of Tanaka *et al.* (2017) are consistent with those of Sakoda *et al.* (2020) at temperatures above 350 K, but at lower temperatures the data show slightly positive deviations up to 0.55 %. Systematic positive deviations are observed in the data of Boonaert *et al.* (2020). The largest deviation in the data is 1.64 % at 283 K. The data of Kimura (2019) are inconsistent with the other datasets.

3.2 Saturated liquid and vapor densities

In Figure 2, the saturation boundary calculated from the equation of state is plotted on a T - ρ diagram, along with experimental data of the saturated liquid and vapor densities (Sakoda *et al.*, 2020). The calculated boundary reasonably represents the experimental data. The average deviations are 0.72 % for the saturated liquid densities and 0.69 % for the saturated vapor densities, which are quite acceptable, although they exceed the experimental uncertainties claimed by the authors (0.06–0.24 %, $k = 2$). The rectilinear diameter, the mean value of saturated liquid and vapor densities, is almost straight up to the critical temperature.

3.3 (p, ρ, T) behavior

The data measured by Sakoda *et al.* (2020) based on the isochoric method are the only available dataset for the (p, ρ, T) behavior of R1336mzz(E). Their typical experimental uncertainty in density is 0.15 % ($k = 2$). Relative density deviations in the data from calculated values with the equation of state are given in Figure 3. The overall average deviation is 0.20 %, and 23 data points out of 40 data are represented within the uncertainty. The vapor isochores (52, 123, and 200 kg m⁻³) show systematic negative deviations, which gradually become larger as temperature and pressure increase. The maximum and average deviations are 0.53 % and 0.32 %. The liquid densities along two isochores of 1061 and 1212 kg m⁻³ are well represented, but those along an isochore of 924 kg m⁻³ show larger deviations. The maximum and average deviations are 0.72 % and 0.13 %.

3.4 Sound speed

Kano *et al.* (2019) measured vapor-phase sound speeds with a cylindrical resonator, which is the only available dataset for the sound speed of R1336mzz(E). Their experimental uncertainties are 0.1 % at maximum. Figure 4 shows deviations in the data from calculated values with the equation of state. The data are accurately represented by the equation, and no systematic deviations are observed. The maximum and average deviations are 0.044 % and 0.017 %.

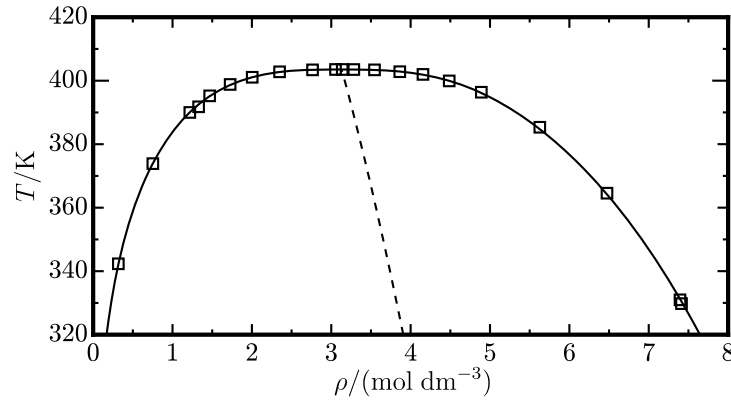


Figure 2: Saturation boundary calculated from the equation of state and experimental data of the saturated liquid and vapor densities: (□) Sakoda *et al.* (2020); The dashed line indicates the rectilinear diameter.

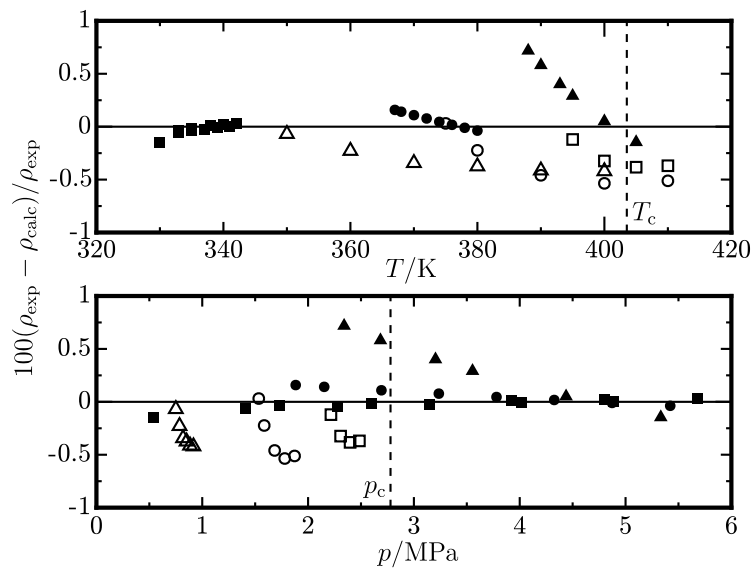


Figure 3: Relative density deviations in the (p, ρ, T) data of Sakoda *et al.* (2020) from calculated values with the equation of state: (Δ) 52 kg m⁻³; (○) 123 kg m⁻³; (□) 200 kg m⁻³; (▲) 924 kg m⁻³; (●) 1061 kg m⁻³; (■) 1212 kg m⁻³.

4. BEHAVIOR IN THE CRITICAL AND EXTRAPOLATED REGIONS

Derived properties calculated from higher-order partial derivatives of the Helmholtz energy are generally sensitive to underlying problems in equations of state, and therefore their plots on various thermodynamic coordinates are often used to verify the behavior of the equations in the critical and extrapolated regions. A few examples are shown here.

Virial coefficients are the most elemental properties, and their values, slopes, and curvatures were constrained while fitting in this work. Figure 5 shows changes in the third and fourth virial coefficients (C and D) calculated from the equation of state; they are related to the second and third derivatives of the Helmholtz energy with respect to density:

$$C = \lim_{\delta \rightarrow 0} \left[\frac{1}{\rho_c^2} \left(\frac{\partial^2 \alpha^r}{\partial \delta^2} \right)_{\tau} \right] \quad (5)$$

and

$$D = \lim_{\delta \rightarrow 0} \left[\frac{1}{2\rho_c^3} \left(\frac{\partial^3 \alpha^r}{\partial \delta^3} \right)_{\tau} \right]. \quad (6)$$

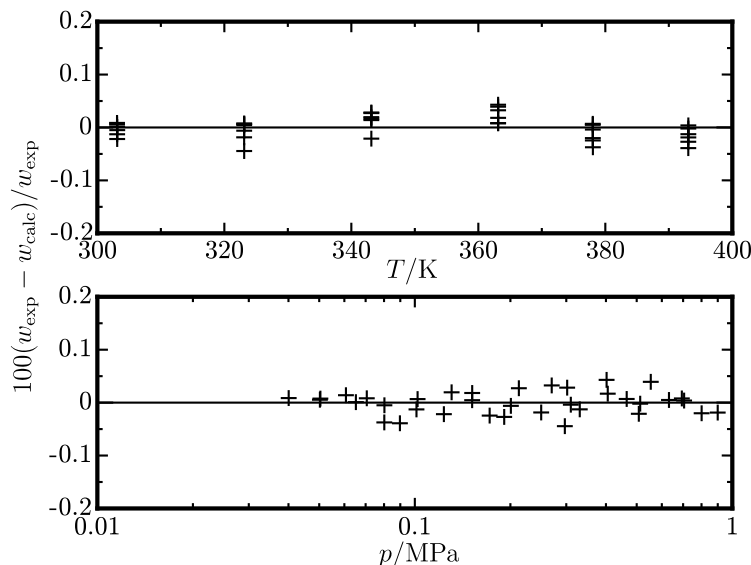


Figure 4: Relative deviations in experimental vapor-phase sound speed data from calculated values with the equation of state: (+) Kano *et al.* (2019).

Based on an equation of state for Lennard-Jones fluids, Thol *et al.* (2016) demonstrated the theoretically expected changes in the virial coefficients over a wide range of temperature. They qualitatively agree with the behavior of C and D observed in Figure 5.

Figure 6 shows the residual isochoric heat capacities $c_v^r (= c_v - c_v^\circ)$ versus temperature along the saturation lines, isobars, and the critical isochore. This figure demonstrates reasonable behavior of the equation of state not only within the range of the experimental data, but also for extrapolated states at higher temperatures and pressures, and lower temperatures. The critical isochore monotonically decreases from the critical point to higher temperatures, which means that temperature derivatives of the residual Helmholtz energy are properly formulated because the isochoric heat capacity is calculated only from the second partial derivative of the Helmholtz energy with respect to temperature.

The phase identification parameter (PIP) (Venkatarathnam & Oelrich, 2011), which was originally used to distinguish whether a state point is in the vapor or liquid phase, can highlight incorrect behavior in an equation of state because it is calculated from several higher-order derivatives of the Helmholtz energy. The PIP is defined as

$$\text{PIP} = 2 - \rho \left[\frac{\partial^2 p}{\partial \rho \partial T} - \frac{\left(\frac{\partial^2 p}{\partial \rho^2} \right)_T}{\left(\frac{\partial p}{\partial T} \right)_\rho} - \frac{\left(\frac{\partial p}{\partial \rho} \right)_T}{\left(\frac{\partial p}{\partial \rho} \right)_T} \right]. \quad (7)$$

Figure 7 shows the PIP calculated from the equation of state versus temperature along isobars from 0.5 MPa to 1000 MPa. The saturation lines and isobars are smooth over wide ranges of temperature and pressure, and no unreasonable behavior is observed, as seen in the PIP behavior of published equations of state.

5. CONCLUSIONS

The Helmholtz energy equation of state for R1336mzz(E) presented here is valid for temperatures from 287 K to 410 K and pressures up to 5.7 MPa. Comparisons to the experimental data concluded that expected relative uncertainties ($k = 2$) in this range are 0.1 % for vapor pressures, 1 % for saturated liquid densities, 1 % for saturated vapor densities, 0.15 % for liquid densities, 0.5 % for vapor densities, and 0.05 % for vapor-phase sound speeds, except in the critical region where larger uncertainties of up to 2 % are sometimes observed in densities. Plots of various derived properties show that the equation exhibits reasonable behavior in the critical and extrapolated regions. The equation will be available in the next version of REFPROP (Lemmon *et al.*, 2018). We plan to update the equation when additional measurements become available.

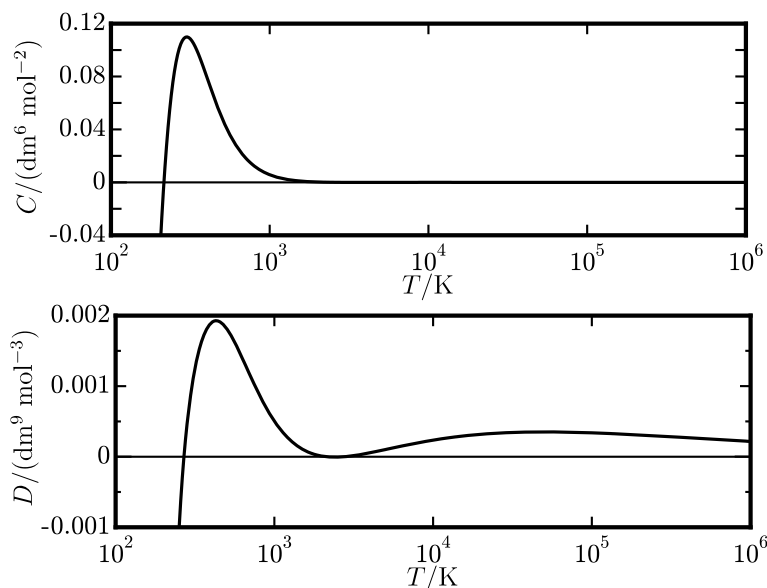


Figure 5: Third and fourth virial coefficients (C and D) calculated from the equation of state.

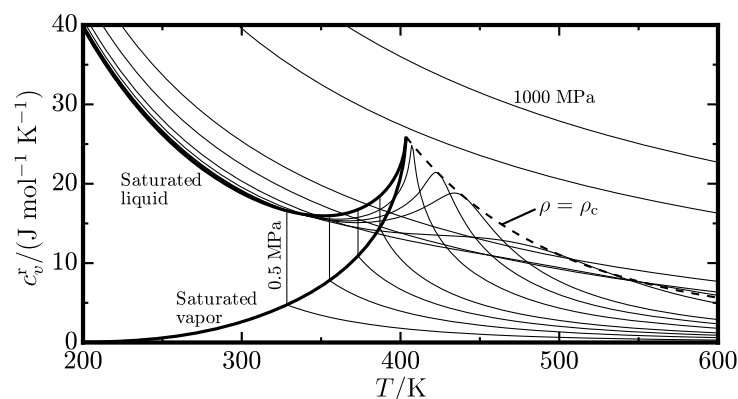


Figure 6: Residual isochoric heat capacity (c_v^r) versus temperature along isobars at 0.5, 1, 1.5, 2, 3, 4, 5, 10, 20, 50, 100, 500, and 1000 MPa, and the critical isochore ($\rho = \rho_c$).

REFERENCES

- Akasaka, R., Higashi, Y., Sakoda, N., Fukuda, S., & Lemmon, E. W. (2020). Thermodynamic properties of trifluoroethene (R1123): (p, ρ, T) behavior and fundamental equation of state. *Int. J. Refrig.*, *119*, 457–467. doi: 10.1016/j.ijrefrig.2020.07.011
- Akasaka, R., & Lemmon, E. W. (2019). Fundamental equations of state for cis-1,3,3,3-tetrafluoropropene [R-1234ze(Z)] and 3,3,3-trifluoropropene (R-1243zf). *J. Chem. Eng. Data*, *64*(11), 4679–4691. doi: 10.1021/acs.jced.9b00007
- Akasaka, R., Lemmon, E. W., Simoni, L. D., & Huber, M. L. (2022). to be submitted to *Int. J. Thermophys.*
- Boonaert, E., Valtz, A., Brocus, J., Coquelet, C., Beucher, Y., De Carlan, F., & Fourmigué, J.-M. (2020). Vapor-liquid equilibrium measurements for 5 binary mixtures involving HFO-1336mzz(E) at temperatures from 313 to 353 K and pressures up to 2.735 MPa. *Int. J. Refrig.*, *114*, 210–220. doi: 10.1016/j.ijrefrig.2020.02.016
- Juhasz, J. R. (2017). Novel working fluid, HFO-1336mzz(E), for use in waste heat recovery application. In *Proceedings of the 12th IEA heat pump conference*. Rotterdam, the Netherlands.
- Kano, Y., Kayukawa, Y., & Fujita, Y. (2019). Speed of sound and dielectric constant measurements for HFO-1336mzz(E) in the gas phase. In *Proceedings of the 2nd Pacific rim thermal engineering conference*. Hawaii,

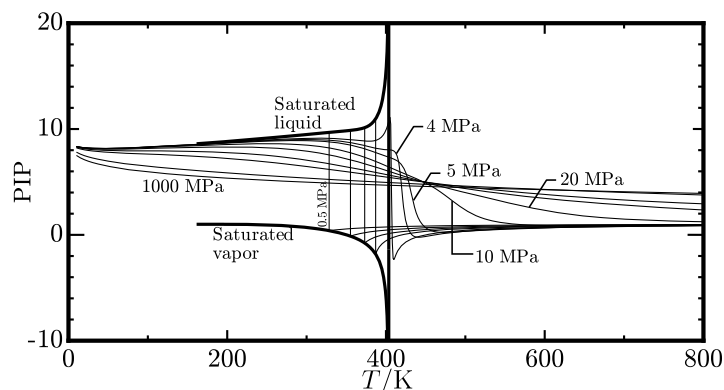


Figure 7: Phase identification parameter (PIP) versus temperature along isobars at 0.5, 1, 1.5, 2, 3, 4, 5, 10, 20, 50, 100, 500, and 1000 MPa.

USA.

- Kayukawa, Y., Kondou, C., Sakoda, N., Kariya, K., & Fukuda, S. (2021). *JSRAE Thermodynamic Tables JARef Vol. 5: HFOs & HCFOs*. Japan Society of Refrigerating and Air Conditioning Engineers.
- Kedzierski, M. A., & Lin, L. (2020). *Pool boiling of R514A, R1224yd(Z), and R1336mzz(E) on a reentrant cavity surface; extensive measurement and analysis*. National Institute of Standards and Technology.
- Kimura, T. (2019). *Thermodynamic properties of HFO refrigerants as working fluid for high temperature heat pump*. Unpublished doctoral dissertation, Waseda University, Japan.
- Lemmon, E. W., Bell, I. H., Huber, M. L., & McLinden, M. O. (2018). *NIST Standard Reference Database 23: Reference Fluid Thermodynamic and Transport Properties-REFPROP, Version 10.0*, National Institute of Standards and Technology. Retrieved from <https://www.nist.gov/srd/refprop> doi: 10.18434/T4JS3C
- Lemmon, E. W., McLinden, M. O., & Wagner, W. (2009). Thermodynamic properties of propane. III. A reference equation of state for temperatures from the melting line to 650 K and pressures up to 1000 MPa. *J. Chem. Eng. Data*, 54(12), 3141–3180. doi: 10.1063/1.556054
- Mondal, D., Kariya, K., Tuhin, A. R., Amakusa, N., & Miyara, A. (2022). Viscosity measurement for *trans*-1,1,1,4,4,4-hexafluoro-2-butene (R1336mzz(E)) in liquid and vapor phases. *Int. J. Refrig.*, 133, 267–275.
- Mondal, D., Kariya, K., Tuhin, A. R., Miyoshi, K., & Miyara, A. (2021). Thermal conductivity measurement and correlation at saturation condition of HFO refrigerant *trans*-1,1,1,4,4,4-hexafluoro-2-butene (R1336mzz(E)). *Int. J. Refrig.*, 129, 109–117.
- Murphy, D. L., & Katancik, M. S. (2021). Miniature oil-less reciprocating compressor for high-lift, high-temperature heat pump applications. In *Proceedings of 25th international compressor engineering conference at Purdue (PaperID 2681)*. West Lafayette, IN, USA.
- Sakoda, N., Higashi, Y., & Akasaka, R. (2020). Measurements of *PvT* properties, vapor pressures, saturated densities, and critical parameters for *trans*-1,1,1,4,4,4-hexafluoro-2-butene (R1336mzz(E)). *J. Chem. Eng. Data*, 66(1), 734–739. doi: 10.1021/acs.jced.0c00848
- Tanaka, K., Ishikawa, J., & Kontomaris, K. K. (2017). Thermodynamic properties of HFO-1336mzz(E) (*trans*-1,1,1,4,4,4-hexafluoro-2-butene) at saturation conditions. *Int. J. Refrig.*, 82, 283–287. doi: 10.1016/j.ijrefrig.2017.06.012
- Thol, M., Rutkai, G., Köster, A., Lustig, R., Span, R., & Vrabec, J. (2016). Equation of state for the Lennard-Jones fluid. *J. Phys. Chem. Ref. Data*, 45(2). doi: 10.1063/1.4945000
- Tiesinga, E., Mohr, P. J., Newell, D. B., & Taylor, B. N. (2021). CODATA recommended values of the fundamental physical constants: 2018. *J. Phys. Chem. Ref. Data*, 50(3), 033105. doi: 10.1063/5.0064853
- Tomassetti, S., Di Nicola, G., & Kondou, C. (2022). Triple point measurements for new low-global-warming-potential refrigerants: Hydro-fluoro-olefins, hydro-chloro-fluoro-olefins, and trifluoriodomethane. *Int. J. Refrig.*, 133, 172–180. doi: 10.1016/j.ijrefrig.2016.02.003
- Venkatarathnam, G., & Oellrich, L. R. (2011). Identification of the phase of a fluid using partial derivatives of pressure, volume, and temperature without reference to saturation properties: Applications in phase equilibria calculations. *Fluid Phase Equilib.*, 301(4), 225–233. doi: 10.1016/j.fluid.2010.12.001